Fuel 357 (2024) 129815

Contents lists available at ScienceDirect

Fuel

journal homepage: www.elsevier.com/locate/fuel

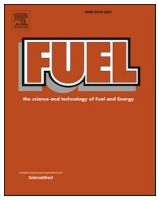

Full Length Article

Fuelling the future: Unleashing energy and exergy efficiency from municipal green waste pyrolysis

M.M. Hasan [a,*], M.G. Rasul [a], M.I. Jahirul [a], M. Mofijur [b,c]

[a] School of Engineering and Technology, Central Queensland University, QLD 4701, Australia
[b] Centre for Technology in Water and Wastewater, School of Civil and Environmental Engineering, University of Technology Sydney, Ultimo, NSW 2007, Australia
[c] Mechanical Engineering Department, Prince Mohammad Bin Fahd University, Al Khobar 31952, Saudi Arabia

ARTICLE INFO

Keywords:
Fast pyrolysis
Municipal green waste
Sustainable fuel
Bio-oil
Energy analysis
Exergy analysis

ABSTRACT

This study aims to determine how different operating conditions for a fast pyrolysis process employing municipal green waste (MGW) in an auger reactor affect product yields, overall energy efficiency, and total exergy efficiency. In this study, a range of pyrolysis conditions, including temperatures from 400 to 600 °C (in 50 °C increments), holding times from 1 to 5 min (in 1-minute increments), and feedstock particle sizes from 2 to 10 mm (in 2-mm increments) were used. MGW and pyrolysis products were characterised using separate pieces of equipment and in accordance with applicable ASTM standards. The results demonstrate that a yield of 52.8% for bio-oil and a yield of 23.7% for syngas can be achieved at temperatures of 500 and 600 °C, respectively. At 400 °C, the biochar production was highest as 21.5%. Bio-oil and syngas yields improved with holding times, whereas biochar yields declined. At a feedstock particle size of 2 mm, the overall energy efficiency was at its maximum (72.9%), while the total exergy efficiency was also at its highest (68.4%). As feedstock particle size increased, overall energy efficiency and total exergy efficiency dropped. In conclusion, this study provides valuable insights into the effects of different operating parameters on the pyrolysis process using MGW, which can be used to optimize the process and increase its efficiency.

1. Introduction

The global need for secure and sustainable energy sources, coupled with the urgency to address climate change and the gradual depletion of fossil fuel reserves, has triggered a significant shift towards renewable energy options [1]. Among these alternatives, biofuels have emerged as a particularly promising solution for the transportation sector as they offer the potential to replace conventional fossil fuels [2]. In this context, municipal green waste (MGW), also referred to as organic waste, has garnered considerable attention as a valuable resource for renewable energy generation due to its abundance and cost-effectiveness [3]. Out of various biomass sources, municipal green waste has emerged as a leading contender for biofuel production, owing to its impressive energy content and environmentally neutral characteristics [4]. To harness its potential, pyrolysis has emerged as a highly promising conversion method, involving the application of high temperatures to biomass in the absence of oxygen. This process yields valuable by-products such as bio-oil, biochar, and syngas [5]. However, despite its promise, the commercial utilization of biofuels derived from municipal green waste is currently restricted due to low yields and suboptimal energy efficiency [6]. Consequently, enhancing the efficiency of the pyrolysis process becomes crucial in order to improve its economic viability.

The pyrolysis process encompasses various techniques including slow, fast, and flash pyrolysis. Of particular interest among these is the fast pyrolysis process, which has garnered significant attention due to its capability to yield a larger quantity of bio-oil compared to the other two methods [7]. Notably, the liquid nature of the primary output from fast pyrolysis simplifies its storage and transportation [8]. Recent literature [9–12] highlights the growing interest in advancing fast pyrolysis techniques, with a focus on enhancing bio-oil yields, quality, and process efficiency. This renewed attention has led to innovative reactor designs and operational improvements. Among the available reactor options, the auger-type reactor has gained prominence for its straightforward handling and operational procedures [13]. The auger reactor's inherent advantages have positioned it as one of the most promising reactor configurations for the fast pyrolysis process, offering efficient heat and mass transfer mechanisms. In the context of recent progress,

* Corresponding author.
E-mail address: m.m.hasan@cqu.edu.au (M.M. Hasan).

https://doi.org/10.1016/j.fuel.2023.129815
Received 16 May 2023; Received in revised form 28 August 2023; Accepted 11 September 2023
Available online 15 September 2023

substantial developments have been observed in the design and performance of auger reactors for fast pyrolysis. Researchers have been investigating modifications to auger reactor geometry [14], feedstock preparation techniques [15], and process parameters [16] to optimize bio-oil yield and quality. These advancements have been complemented by computational modelling and simulation studies, contributing to a deeper understanding of the complex heat and mass transfer dynamics within auger reactors. Reflecting this progress, a pilot-scale auger pyrolysis reactor was chosen as the focal point of this study.

Energy and exergy analyses play a crucial role in assessing the efficiency of the fast pyrolysis process [17]. Energy analysis provides valuable insights into the overall energy input and output of the process, while exergy analysis delves deeper into the quality of the energy involved. By conducting these analyses, it becomes possible to pinpoint the sources of energy and exergy losses within the process and devise strategies to mitigate them. This, in turn, can lead to enhanced process efficiency and increased production of valuable outputs like bio-oil, biochar, and syngas. Several factors exert influence on the efficiency of MGW fast pyrolysis, including key operating parameters such as temperature, holding time, and feedstock particle size. Selecting the appropriate operating parameters is critical in obtaining high-quality energy products and improving the energy and exergy efficiency of the pyrolysis process. Generally, higher temperatures yield higher energy and exergy efficiencies since more of the feedstock is converted into valuable products. However, it is important to avoid excessively high temperatures that can result in thermal degradation and reduced efficiency [18]. The holding time, representing the duration the feedstock remains inside the reactor, also significantly impacts energy and exergy efficiency. Longer holding times tend to enhance efficiency by increasing the conversion of feedstock. However, the optimal holding time may vary depending on specific process conditions [19]. Another factor to consider is the feedstock particle size, which can have a notable effect on energy and exergy efficiency. Smaller particle sizes generally lead to improved efficiency due to the increased surface area and enhanced heat transfer. Nevertheless, extremely small particle sizes can give rise to issues like clogging and reduced reactor performance [20].

Several studies have investigated the influence of different operating parameters on the energy and exergy efficiency of biomass fast pyrolysis, yielding valuable insights. For instance, Wang et al. [21] examined the energy and exergy analyses of rice husk pyrolysis products at high temperatures ranging from 800 to 1200 °C. Their findings revealed that the energy and exergy efficiencies of syngas increased as the temperature rose, reaching their highest values at 900 °C. Similarly, Greco et al. [22] explored the impact of temperature on the total exergy efficiency of the pyrolysis process using wheat straw. Their results demonstrated that the exergy efficiency of biomass pyrolysis improved with increasing temperature, peaking at 550 °C with a maximum exergy efficiency of 60.38%. In the realm of holding time, Trubetskaya et al. [23] delved into the effect of this parameter on the energy efficiency of biomass pyrolysis. They discovered that the energy efficiency increased as the holding time extended up to 30 min. However, beyond this threshold, the efficiency declined due to the accumulation of tar in the reactor. In another investigation concerning crop residues, Hong et al. [24] specifically examined the influence of feedstock particle size on the energy efficiency of the pyrolysis process. Their findings revealed that reducing the particle size from coarse grinding to fine grinding resulted in an increase in energy efficiency. However, further reduction to ultrafine grinding led to diminished efficiency, potentially due to excessive volatiles release. The existing literature indicates a scarcity of comprehensive studies on the fast pyrolysis of MGW utilizing an auger reactor, especially concerning energy and exergy analysis. Given this gap, investigating the synergy between the auger reactor, MGW, and fast pyrolysis represents a promising avenue. This endeavour stands to significantly enhance our understanding of this domain by introducing novel insights and knowledge.

This study aims to examine the effects of various operating parameters, including temperature, holding time, and feedstock particle size, on the energy and exergy efficiency of MGW fast pyrolysis. While previous studies have explored the impact of these parameters on the pyrolysis process, our study's novelty lies in its specific focus on fast pyrolysis of MGW, an area that has received relatively less attention in research. The findings of this study will offer valuable insights into optimizing the fast pyrolysis process for the efficient production of biofuels from MGW.

2. Materials and methods

2.1. Material

The MGW used in this study was collected from the Waste Transfer Station located in Rockhampton, Queensland, Australia, following the American Society for Testing and Materials (ASTM) standard E 871–82. To comply with the standard, at least 10 kg of waste must be collected, and around 40 kg of MGW was collected for this study. The collected MGW consisted of hedge trimmings and various parts of trees, including branches, trunks, and stumps, as well as soil and impurities that needed to be removed. Therefore, the MGW was thoroughly cleaned and left to dry in the sun for 12 days. After that, it was shredded into required sizes of 2 mm, 4 mm, 6 mm, 8 mm, and 10 mm using a shredder, and sun-dried again to reduce the moisture content. To ensure uniformity, the shredded materials were blended before being fed into the reactor. Fig. 1 displays the collected and shredded MGW.

2.2. Pyrolysis experiment

To conduct the fast pyrolysis of MGW, an auger reactor was used in the Fuel and Energy Research Laboratory situated at the North Rockhampton campus of Central Queensland University, Australia. The reactor was comprised of four main sections, namely, the feeder, the reactor part, the biochar vessel, and the condenser, as shown in Fig. 2. The reactor part is constructed from a quartz tube and is heated externally using three electrical ring furnaces. This part is sealed with an insulation sheet on the outside. The length of this reactor part measures 1300 mm, and its outer diameter is 100 mm. The reactor has a volume of 20 L, while the feeding section holds 5 L. Moving on to the condenser, it spans a length of 800 mm and covers an area of 1 m^2. Our previous work [25] provides a detailed description of the auger reactor and the time–temperature profile of the fast pyrolysis process. In each pyrolysis experiment, 2 kg of MGW was used and the reactor system was nitrogen-purged for 15 min to remove any oxygen. The reactor was then heated to the desired temperature. Once this temperature was reached, the auger motor was activated to move the feedstock from one end of the reactor to the other. The speed of the auger rotation controlled how long the feedstock stayed inside the reactor, i.e., the holding time of the

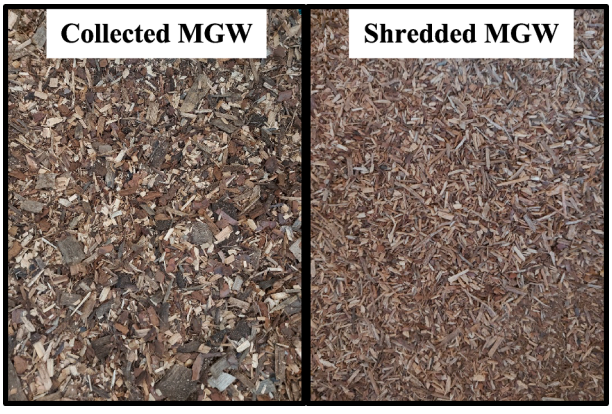

Fig. 1. Photographs of collected and shredded MGW.

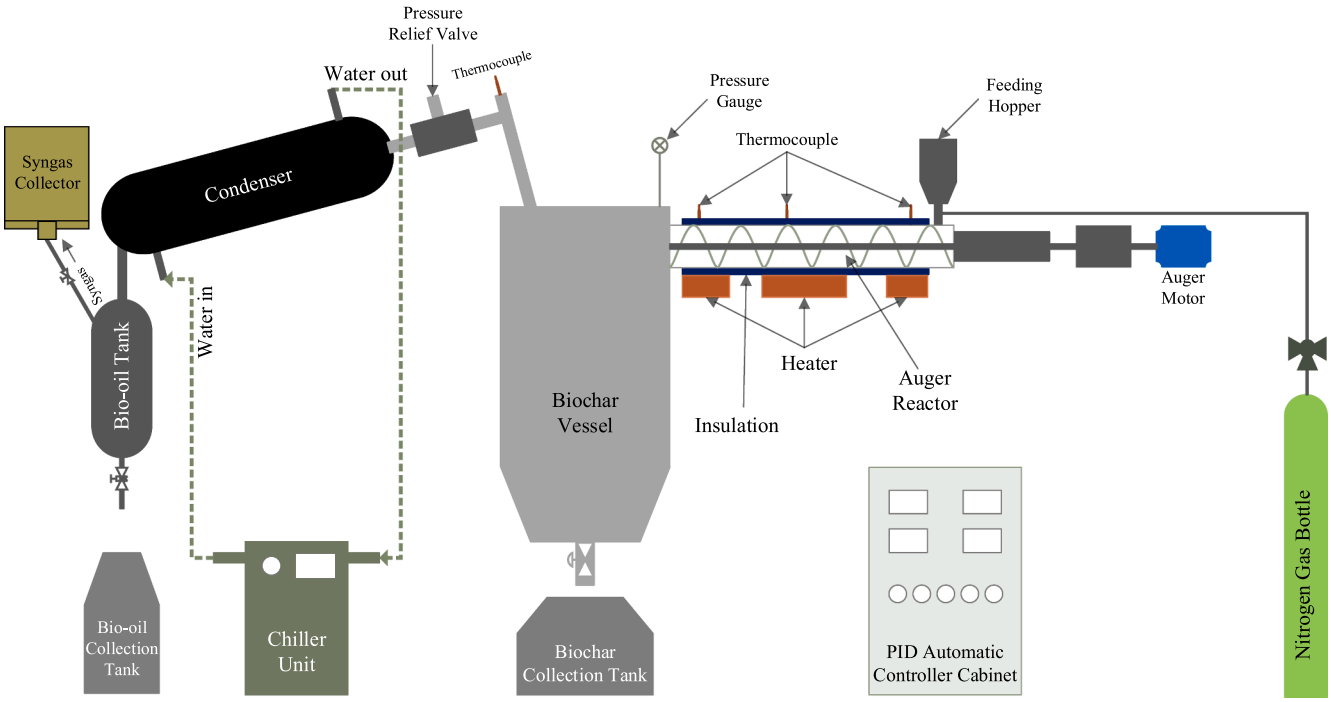

Fig. 2. The schematic diagram of the pyrolysis setup used in the present study.

feedstock. While the auger transported the feedstock, it was heated at a rate of 30 °C/s until it reached the specific pyrolysis temperature. This led to the fast pyrolysis of MGW inside the reactor, resulting in the production of two products: biochar and vapor. After the process, the biochar was collected in a separate tank and the vapour was condensed. The syngas, which is a non-condensable pyrolysis product, was released through an exhaust valve and collected in a sample collection bag while the bio-oil, which is the condensable product, was collected in a separate tank. Each experiment was repeated three times with distinct samples, and the mean data were analysed. The experimental matrix is shown in Table 1. As evident from the Table 1, while one parameter was varied, the other two remained consistent. The selection of experimental conditions such as range of each parameter and constant values for other 2 parameters was determined by two criteria. The first criterion drew from data collected in our previous experiments involving similar materials [4,16,25], while the second relied on insights gleaned from a comprehensive literature review.

The product yields were calculated according to the following equations:

$$Yieldofbio-oil(\%) = \frac{Massofbio-oil}{Massoffeedstock} \times 100 \quad (1)$$

$$Yieldofbiochar(\%) = \frac{Massofbiochar}{Massoffeedstock} \times 100 \quad (2)$$

$$Yieldofsyngas(\%) = 100 - (Yieldofbio-oil + Yieldofbiochar) \quad (3)$$

2.3. Characterisation of feedstock and pyrolysis products

Characterizing MGW and biochar is crucial for understanding their chemical composition. Proximate analysis, ultimate analysis, and higher heating value (HHV) measurements are commonly employed techniques for this purpose. In this study, proximate analysis of the samples was conducted according to the ASTM D3173 standard method, utilizing a Thermogravimetric Analyzer (TGA) - PerkinElmer Pyris Diamond TGA. This analysis determined the moisture content, ash content, volatile matter, and fixed carbon present in the MGW and biochar samples. To assess the elemental composition of the samples, ultimate analysis was performed using a CHN analyzer - PerkinElmer 2400 Series II CHNS/O Elemental Analyzer. This analysis provided information on the carbon, hydrogen, nitrogen, sulfur, and oxygen content of the MGW and biochar samples. Furthermore, the HHV of the samples was measured using a bomb calorimeter - Parr 1261 Oxygen Bomb Calorimeter. This measurement quantified the amount of energy released when the samples underwent complete combustion.

In this study, elemental analysis of the bio-oil sample was performed using a CHN analyser - PerkinElmer 2400 Series II CHNS/O Elemental Analyser. The analysis involved measuring the carbon, hydrogen, nitrogen, and sulfur content of the bio-oil. The oxygen content was calculated by difference, as the sum of the carbon, hydrogen, nitrogen, and sulfur content should add up to 100% on a weight basis. The elemental composition of bio-oil is crucial in determining its fuel properties, such as calorific value, viscosity, and stability. The CHN analyser provided accurate and reliable results, which helped understand the chemical composition and properties of the bio-oil sample. Standardized methods, such as ASTM D5291, were followed to ensure the accuracy and reliability of the results.

The composition analysis of the syngas was carried out in this study using Gas Chromatography (GC) - Agilent 7890B GC equipped with a thermal conductivity detector (TCD) and a flame ionization detector (FID). The analysis involved separating the individual gas components in the syngas and measuring their respective concentrations. Gas composition analysis is a crucial technique for characterizing the quality and composition of syngas produced from fast pyrolysis of MGW. The GC analysis identified and quantified the major gas components in the syngas, such as hydrogen (H_2), carbon monoxide (CO), carbon dioxide (CO_2), and methane (CH_4). The GC analysis was carried out following ASTM D1945 standard method, which outlines procedures for the

Table 1
The experimental matrix used in the present study.

Matrix	Temperature (°C)	Holding time (min)	Particle size (mm)
1	400 – 600	3	2
2	550	1 – 5	2
3	550	3	2 – 10

determination of the composition of the gas mixture using a GC. The use of a TCD and FID detector allowed for accurate and reliable measurements of the gas concentration.

2.4. Energy analysis

The energy analysis of the fast pyrolysis process of MGW involves the calculation of the energy input required to heat the feedstock, the energy output in the form of products, and the overall energy efficiency of the process.

Energy input in the pyrolysis process can be calculated using the Equation 1 [26]:

$$\text{Energy input (MJ/kg)},\ E_{in} = Q_s + Q_{mgw} \tag{1}$$

where: Q_s is the energy required to heat the pyrolysis feedstock and to transform the feedstock into pyrolysis products in MJ/kg and Q_{mgw} is the energy contained in MGW in MJ/kg. Q_{mgw} can be calculated using Equation 2:

$$Q_{mgw} = HHV_{mgw} \tag{2}$$

where: HHV_{mgw} is the HHV of MGW in MJ/kg.

Energy output in the pyrolysis process can be calculated using the Equation 3 [27]:

$$\text{Energy output (MJ/kg)}, E_{out} = Q_l + Q_c + Q_g \tag{3}$$

where: Q_l is the energy contained in bio-oil in MJ/kg, Q_c is the energy contained in biochar in MJ/kg, and Q_g is the energy contained in syngas in MJ/kg. Q_l, Q_c and Q_g can be calculated using the following Equations:

$$Q_l = M_l \times HHV_l \tag{4}$$

$$Q_c = M_c \times HHV_c \tag{5}$$

$$Q_g = M_g \times HHV_g \tag{6}$$

where: M_l, M_c and M_g are the mass yields of bio-oil, biochar, and syngas produced, respectively and HHV_l, HHV_c and HHV_g are the higher heating values of bio-oil, biochar, and syngas in MJ/kg, respectively.

The energy balance of the pyrolysis process can be expressed by Equation 7 which is based on the first law of thermodynamics:

$$E_{in} = E_{out} + E_{loss} \tag{7}$$

where: E_{loss} (MJ/kg) is the energy loss in the pyrolysis process.

The overall energy efficiency (η) of the pyrolysis process is the percentage ratio of the energy output to the energy input [21]. It can be represented by the following Equation 8:

$$Overall energy efficiency, \eta = (E_{out}/E_{in}) \times 100\% \tag{8}$$

2.5. Exergy analysis

Exergy analysis is a useful tool for evaluating the efficiency and sustainability of energy conversion processes, including pyrolysis. It involves assessing the potential for useful work that can be obtained from a process, based on the availability of energy and the thermodynamic properties of the system. The exergy balance of the pyrolysis process of MGW can be expressed by Equation 9 which is based on the second law of thermodynamics [28]:

$$e_{mgw} = e_g + e_c + e_l + e_{loss} \tag{9}$$

where: e_{mgw}, e_g, e_c and e_l are the total exergy of MGW, syngas, biochar, and bio-oil in MJ/kg, respectively. e_{loss} is the exergy loss of pyrolysis process in MJ/kg.

The total exergy of a certain component is expressed by the sum of different types of exergies and is written as Equation 10 [29]:

$$\text{Total exergy (MJ/kg)}, e_x = e_x^{ph} + e_x^{ch} + e_x^{ki} + e_x^{po} \tag{10}$$

where: e_x^{ph}, e_x^{ch}, e_x^{ki} and e_x^{po} are physical, chemical, kinetic, and potential exergy in MJ/kg, respectively.

According to Wang et al. [21], the kinetic and potential exergy can be neglected as their values are relatively small. So, Equation 10 can be expressed as following:

$$\text{Total exergy (MJ/kg)}, e_x = e_x^{ph} + e_x^{ch} \tag{11}$$

The physical exergy of syngas is calculated as follows [30]:

$$e_g^{ph} = \sum n_i[(h - h_0) - T_0(s - s_0)] \tag{12}$$

$$h - h_0 = \int_{T_0}^{T} C_p dT \tag{13}$$

$$s - s_0 = \int_{T_0}^{T} \frac{C_p}{T} dT \tag{14}$$

where: n_i represents the molar yield of syngas component i in mol/kg, while h and s refer to the specific enthalpy and specific entropy of gas component i under the operating conditions, expressed in kJ/kmol and kJ/kmol-K, respectively. Additionally, h_0 and s_0 denote the specific enthalpy and specific entropy of gas component i at standard condition. Finally, C_p is the constant pressure specific heat capacity of gas component i, expressed in J/mol-K.

C_p is calculated by an empirical correlation as Equation 15:

$$C_p = A + BT + CT^2 + DT^4 \tag{15}$$

where: A, B, C, and D are the coefficients of C_p at constant pressure and presented in Table 2.

The chemical exergy of syngas is calculated using the following Equation 16 [31]:

$$e_g^{ch} = \sum y_i e_{ch,i}^0 + T_0 R \sum y_i ln y_i \tag{16}$$

The Equation 16 includes the following variables: y_i, which represents the mole fraction of gas component i; $e_{ch,i}^0$, which denotes the standard chemical exergy of gas component i in kJ/kmol (as listed in Table 3); and R, which is the general gas constant with a value of 8.3144 J/mol-K.

According to Zhang et al. [32], the physical energy of char, bio-oil and MGW can be ignored. So, these values were not calculated in this study. The chemical exergy of bio-oil, biochar, and MGW can be calculated by following equations:

$$e_l = \beta_0 \times LHV_l \tag{17}$$

$$e_c = \beta_1 \times LHV_c \tag{18}$$

$$e_{mgw} = \beta_1 \times LHV_{mgw} \tag{19}$$

where: LHV_l, LHV_c, and LHV_{mgw} are the lower heating values of bio-oil, biochar, and MGW in MJ/kg, respectively. β_0 is the correlation factor of

Table 2
The coefficients of C_p at constant pressure of different components of syngas obtained from the fast pyrolysis of MGW.

Syngas component	A	B	C	D	Temperature (K)
H_2	29.11	−0.192	0.4	−0.87	273–1800
CO	28.16	0.168	0.533	−2.222	273–1800
CO_2	22.26	5.981	−3.501	7.469	273–1800
CH_4	19.89	5.024	1.269	−11.01	273–1800

Table 3
The standard chemical exergy of different components of syngas obtained from the fast pyrolysis of MGW.

Syngas component	$e^0_{ch,i}$(kJ/kmol)
H_2	236,100
CO	275,100
CO_2	19,870
CH_4	831,650

bio-oil and β_1 is the correlation factor of both biochar and MGW. The correlation factor β can be defined as the ratio of the actual exergy of a substance to the maximum possible exergy that it could have if it were in equilibrium with the reference environment [33]. The physical meaning of β, in this case, is to represent the proportion of the exergy of a substance that can be converted into useful work, considering the reference environment (usually the surroundings at ambient conditions) as a baseline. It helps in understanding how efficiently a substance can be converted into useful energy, taking into account the inherent irreversibilities and losses within the system [34]. The factors of β_0 and β_1 are based on ultimate analysis and were calculated using the following equations [21,30]:

$$\beta_0 = 1.0401 + 0.1728\frac{H}{C} + 0.0432\frac{O}{C} \tag{20}$$

$$\beta_1 = \frac{1.044 + 0.0160\frac{H}{C} - 0.3493\frac{O}{C}\left(1 + 0.0531\frac{H}{C}\right) + 0.0493\frac{N}{C}}{1 - 0.4124\frac{O}{C}} \tag{21}$$

where: H, C, O, and N are the mass fraction of hydrogen, carbon, oxygen, and nitrogen on a dry basis.

The total exergy efficiency (ψ) of MGW pyrolysis can be calculated as following [26]:

$$\psi = \frac{e_g + e_c + e_l}{e_{mgw}} \times 100\% \tag{22}$$

3. Results and discussion

3.1. Characteristics of MGW

Proximate and ultimate analyses were performed to fully characterise MGW for the purpose of assessing its potential as a fuel source. These types of analyses are frequently used to determine whether or not a solid material is suitable for use in fuel production. In instance, for bio-oil generation through pyrolysis, a solid material with more volatile matter and lower ash and sulphur content is often considered optimum [4]. Table 4 displays the results of the proximate and ultimate analysis for MGW. Each analysis was conducted three times, and the resulting mean values, along with corresponding measurement errors, are summarized in Table 4. Results are also put in perspective by comparing them to what has been found in prior research on similar materials.

The findings of the proximate analysis demonstrate that the volatile matter content of MGW is quite high (72.68%). Since the pyrolysis process calls for feedstock with a high volatile matter concentration, MGW is a good option [35]. In addition, the ash level of MGW is just 7.91%, which is significantly lower than that of Pistachio soft shell, at 14.21%. As MGW produces less ash during the pyrolysis process, it is an attractive feedstock for this type of energy generation [36]. MGW has a greater carbon content (48.75%) than Pistachio soft shell (45.53%), Wheat straw (42.95%), or Cotton stalk (47.07%), according to ultimate analysis. This high carbon content is a critical factor in the pyrolysis process used to produce bio-oil. Because of its high heating value and potential use as a transportation fuel, the carbon in MGW can be processed into high-quality bio-oil [37]. Compared to Pistachio soft shell (47.17%), Wheat straw (46.99%), and Cotton stalk (42.10%), MGW's low oxygen content (36.85%) shows that it may create higher quality bio-oil through pyrolysis. The quality of the bio-oil produced during the pyrolysis process suffers when oxygen in the feedstock competes with carbon for the available hydrogen [38]. Finally, the HHV of 21.87 MJ/kg was found for MGW, making it a promising feedstock for pyrolysis out of the four materials tested. The HHVs of wheat straw (17.99 MJ/kg), cotton stalk (17.40 MJ/kg), and pistachio soft shell (18.57 MJ/kg) are all lower. MGW has a high heating value since it is rich in carbon and has little ash. It follows that by pyrolysis, MGW could yield a high-quality bio-oil with a high energy density.

Table 4
The proximate analysis, ultimate analysis and HHV of dried MGW in comparison with literature data.

Properties	MGW	Pistachio soft shell [39]	Wheat straw [40]	Cotton stalk [41]
Proximate analysis (% [Error])				
Moisture	0.79 [±0.03]	9.25	–	–
Volatile matter	72.68 [±0.4]	67.85	82.12	76.10
Ash	7.91 [±0.08]	14.21	6.90	5.10
Fixed carbon[a]	18.62 [±0.1]	8.69	10.98	18.80
Ultimate analysis (%[Error])				
C	48.75 [±0.3]	45.53	42.95	47.07
H	7.31 [±0.07]	5.56	5.35	4.58
N	6.28 [±0.06]	1.74	–	1.15
S	0.81 [±0.03]	–	–	–
O[a]	36.85 [±0.3]	47.17	46.99	42.10
HHV (MJ/kg)	21.87 [±0.07]	18.57	17.99	17.40

[a] By difference.

3.2. Yield distribution and composition analysis of pyrolysis products

The effect of temperature on the yields of pyrolysis products derived from MGW is shown in Fig. 3. Three experiments were performed at each temperature and standard deviation is represented by error bars in Fig. 3. It is seen from Fig. 3 that as the temperature increases, the yield of bio-oil also increases. For instance, bio-oil yields are 35.49% at 400 °C

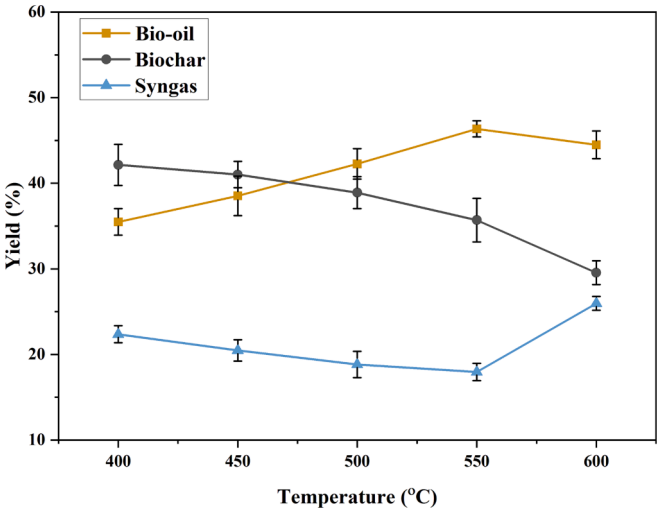

Fig. 3. The effect of temperature on the yields of pyrolysis products derived from the fast pyrolysis of MGW.

and 46.36% at 550 °C. The higher temperatures result in a greater proportion of the feedstock being transformed into liquid products like bio-oil. The complex organic molecules in the feedstock are decomposed by the high temperature, allowing simpler ones to condense and form a liquid [42]. Yet, biochar production falls off sharply as the temperature rises. The output of biochar, for instance, is 42.15% at 400 °C but only 29.54% at 600 °C. The feedstock undergoes mostly dehydration and depolymerization at lower temperatures, leading to a greater production of biochar. However, additional processes like cracking and reforming occur at higher temperatures, further disintegrating the biochar into gases and liquids, and resulting in a decreased biochar output [43]. As the temperature rises from 400 °C to 550 °C, syngas production falls off as well. The production of syngas, for instance, varies from 22.36% at 400 °C to 17.95% at 550 °C. However, the production of bio-oil and syngas changes as the temperature is raised over 550 °C. This is because, above 550 °C, the conversion of biochar and bio-oil into gas phase products becomes more prominent, resulting in a decrease in bio-oil yield and an increase in syngas yield at 600 °C [44].

Fig. 4 depicts the effect of holding time on the yields of pyrolysis products derived from MGW. Three experiments were carried out at various holding times, and the error bars in Fig. 4 depict the standard deviation. It can be observed from Fig. 4 that increasing the holding time results in a higher bio-oil yield. For instance, increasing the holding time from 1 min to 5 min raises the bio-oil yield from 29.24% to 37.31%. Longer holding times allow for a more thorough breakdown of the organic molecules in the feedstock into simpler, smaller molecules, which can condense into bio-oil, hence the correlation between holding time and bio-oil yield [45]. Biochar production, on the other hand, declines with holding time. The biochar yield drops from 54.16% after 1 min of holding time to 44.38% after 5 min of holding time. As biochar is held for prolonged periods of time, it undergoes secondary reactions that further decompose the solid biochar into gases and liquids, resulting in a lower biochar output [46]. Syngas yield decreases somewhat up to a holding time of 2 min, after which it begins to rise again. For instance, increasing the holding time from 1 min to 2 min drops the syngas yield to 15.33% and from 2 min to 5 min increases it to 18.31%. The yield of syngas increases past a specific holding time because the breakdown of syngas into its constituents becomes the dominating process during holding [44]. Bio-oil and biochar yield trends reported at varying holding times are diametrically opposed to pyrolysis trends observed at different temperatures. For instance, in pyrolysis, bio-oil yield increased while biochar yield declined as temperature was increased. This is because the yields of pyrolysis products are affected more by the pyrolysis temperature than by the holding time, or the amount of time the feedstock is subjected to the high temperature.

The yields of bio-oil, biochar, and syngas as a function of MGW particle size is shown in Fig. 5. The pyrolysis experiments were conducted three times using each particle size and the standard deviation is represented by error bars in Fig. 5. The data shows that larger MGW particles result in a lower bio-oil production. For instance, increasing from 2 mm particles to 10 mm particles causes a drop in bio-oil yield from 46.36% to 39.5%. Smaller feedstock particles have a larger surface area per unit mass, which allows for better contact between the feedstock and the heat source, resulting in a more efficient heat transfer and better thermal cracking of the feedstock into bio-oil. This explains why the yield decreases as the particle size of the feedstock increases [47].

On the other hand, larger feedstock particles result in a higher biochar yield. The biochar production, for instance, rises from 35.69% at a particle size of 2 mm to 42.54% at a particle size of 10 mm. Larger feedstock particles need more time to achieve the pyrolysis temperature, therefore they spend more time in the reactor, which leads to a higher biochar yield due to a more thorough conversion of the feedstock into biochar [48]. Syngas production somewhat drops as feedstock particle size increases. For instance, increasing from 2 mm particles to 10 mm particles causes a drop in syngas yield from 17.95% to 14.97%. The longer it takes for larger feedstock particles to reach the pyrolysis temperature and for the gasification reaction to occur, the less syngas they produce throughout the gasification process [49]. The observed patterns in yields of bio-oil, biochar, and syngas with varying feedstock particle size are consistent with trends seen in the literature for similar feedstocks [50–52].

The elemental composition analysis of the pyrolysis products obtained from fast pyrolysis of MGW at various conditions was performed in this study and results are presented in Tables S1, S2 and S3 of the Supplementary Material along with higher heating values. It is seen from Table S1 that increasing the temperature tends to elevate carbon content and HHV while reducing oxygen content, indicating enhanced carbonization and energy content [25]. Holding time variations have minimal impact on elemental composition and HHV, suggesting a relatively rapid attainment of pyrolysis equilibrium. Particle size variations show that smaller particles yield bio-oil with higher carbon content and HHV, indicating better carbonization efficiency [53]. Overall, temperature emerges as the primary factor driving significant changes in bio-oil composition and energy characteristics, offering insights into the key parameters influencing the pyrolysis process of MGW.

Table S2 provides insights into the elemental composition and higher heating values of biochar derived from MGW across varying conditions. Notably, elevating the temperature leads to increased carbon content and higher heating values, coupled with decreased oxygen content, indicating enhanced carbonization and energy density [54]. Holding

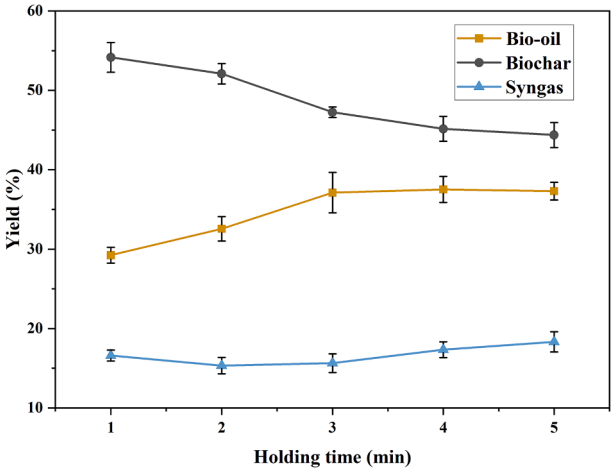

Fig. 4. The effect of holding time on the yields of pyrolysis products derived from the fast pyrolysis of MGW.

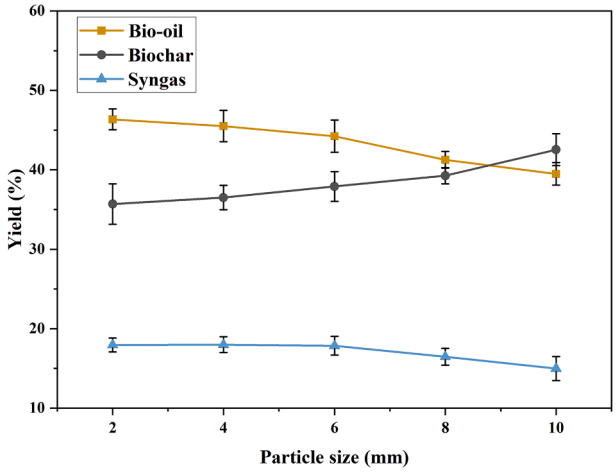

Fig. 5. The effect of particle size on the yields of pyrolysis products derived from the fast pyrolysis of MGW.

time variations exert minimal impact on biochar characteristics, suggesting a swift equilibrium attainment in the pyrolysis process [55]. Particle size variations demonstrate that smaller particle sizes yield biochar with higher carbon content and heating values, implying improved carbonization efficiency [56]. In essence, temperature emerges as the key driver, influencing substantial changes in biochar composition and energy attributes, while holding time and particle size contribute less significantly to these variations.

The trends in species concentration and higher heating values of syngas obtained from MGW across varying conditions is illustrated in Table S3. With increasing temperature, H_2 and CH_4 concentrations rise due to enhanced hydrogen-rich compound formation through pyrolysis and gasification reactions. *CO* concentrations exhibit a slight increase, while CO_2 concentrations decrease, attributed to shifts in gasification equilibria [57]. Holding time and particle size variations have limited impact on syngas properties, reflecting rapid equilibrium attainment and minimal particle size influence. HHV of syngas tend to increase with rising temperature, aligned with the heightened concentrations of hydrogen-rich compounds generated at elevated temperatures [58]. In essence, temperature emerges as the key factor driving substantial changes in the composition and energy attributes of the MGW-derived syngas.

3.3. Effect of temperature on energy and exergy efficiency of MGW pyrolysis process

The effect of temperature on overall energy efficiency and total exergy efficiency of the fast pyrolysis process of MGW is shown in Fig. 6. The standard deviation is represented by error bars in Fig. 6. As can be seen in Fig. 6, the overall energy efficiency of the process improves from 50.34% to 72.89% as the pyrolysis temperature rises from 400 °C to 550 °C and then slightly declines to 71.08% at 600 °C. A higher production of bio-oil, the principal energy product of the process, is anticipated as the pyrolysis temperature rises, as higher temperatures can break down the feedstock more efficiently. As a result, the process becomes more efficient since it produces more usable energy. However, at higher temperatures, the bio-oil output may drop due to more cracking and degradation of the products, which may also lead to greater char formation, thus reducing energy efficiency [59]. Fast pyrolysis of microalgae (*Prosopis juliflora*) biomass was studied by Ramesh and Murugavelh [60] at temperatures between 400 and 600 °C. They found that a rise in pyrolysis temperature from 400 to 600 °C boosted energy efficiency from 43.51 to 59.43%. The present study's findings corroborate this upward trend in energy efficiency. The results of this study are comparable to those of another by Baghel et al. [61], who found an energy efficiency of 84.54% at a pyrolysis temperature of 600 °C.

As pyrolysis temperatures rise from 400 to 600 °C, the process becomes more exergy efficient as a whole. Between 400 and 550 °C, overall exergy efficiency rises from 47.87% to 68.4%, before dropping to 66.3% at 600 °C. The decreased quality of the energy output at higher temperatures is responsible for the drop in total exergy efficiency at 600 °C. The total exergy output of the process drops as the temperature rises because syngas produced at higher temperatures has less exergy due to its lower heating value [62]. With a higher hydrogen content and decreased carbon content, syngas produces less heat when burned. The pyrolysis of wheat straw was studied by Greco et al. [22], who found that increasing the pyrolysis temperature from 400 to 550 °C enhanced the overall exergy efficiency from 50.97 to 60.38%. This is comparable with the present study's findings.

3.4. Effect of holding time on energy and exergy efficiency of MGW pyrolysis process

Fig. 7 shows that the overall energy efficiency and total exergy efficiency of the fast pyrolysis process using MGW at varying holding time. Error bars in Fig. 7 represent the standard deviation. The highest overall energy efficiency of 72.89% and total exergy efficiency of 68.4% are obtained at a holding time of 3 min, while the lowest overall energy efficiency of 52.39% and total exergy efficiency of 48.79% are obtained at a holding time of 1 min. Between 1 and 3 min, energy efficiency and total exergy efficiency both increase with holding time, but then begin to decline with further increasing the holding time. For instance, compared to a holding time of 1 min, the overall energy efficiency climbs to 52.39% after 3 min, but drops to 62.25% after 5 min. Throughout the same range of holding times, overall exergy efficiency goes up from 48.79% to 68.4%, before levelling off at 59.39% after 5 min. There are a few reasons why efficiency rises as holding time increases. Firstly, more efficiency is achieved through a more thorough conversion of the feedstock into energy products during extended holding times [63]. Secondly, the thermal efficiency of the process can be enhanced by increasing the holding time, since this will allow for greater heat transfer from the feedstock to the heating medium [64]. However, inefficiency increases after a particular holding time as a result of things like increasing char formation [65]. Peters et al. [66] carried out a fast pyrolysis study for bio-oil production using lignocellulosic biomass as a feedstock and their findings corroborated with those provided here. Total exergy efficiency was reported to be 71.2%. Overall energy efficiency obtained in the current study is little lower than those found in the presented data, suggesting that the process parameters used in the current investigation were little less effective. However, it is important

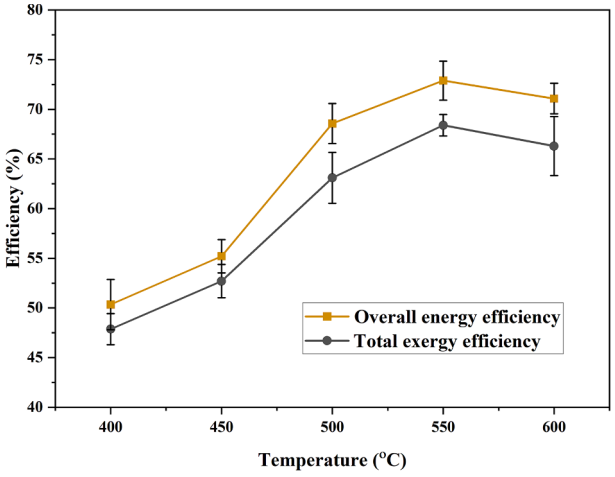

Fig. 6. The effect of temperature on overall energy efficiency and total exergy efficiency of the fast pyrolysis process of MGW.

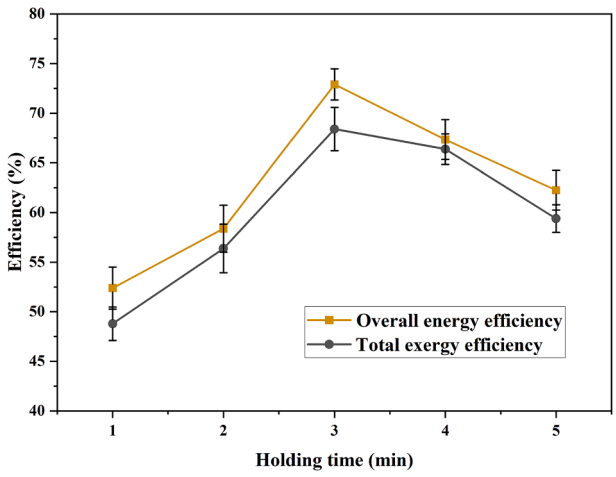

Fig. 7. The effect of holding time on overall energy efficiency and total exergy efficiency of the fast pyrolysis process of MGW.

to note that differences in reported results can be attributed to variations in experimental variables that affect the effectiveness of the fast pyrolysis process. These conditions include feedstock composition, particle size, and reactor design.

3.5. Effect of particle size on energy and exergy efficiency of MGW pyrolysis process

The relationship between overall energy efficiency or total exergy efficiency of fast pyrolysis process of MGW and feedstock particle size is illustrated in Fig. 8. The standard deviation of each measurement is represented by error bar in Fig. 8. As can be clearly observed in Fig. 8 that when feedstock particle size rises, overall energy efficiency and total exergy efficiency tend to decrease. For instance, the overall energy efficiency drops by approximately 25% from 72.89% when dealing with particles of 2 mm in size to 47.49 % when dealing with particles of 10 mm in size. Similarly, the total exergy efficiency drops from 68.4% for 2 mm particles to 43.5% for 10 mm particles, a fall of roughly 25%. Many variables contribute to the decline in energy and total exergy efficiency seen with increasing particle size. To begin, larger particle sizes have a lower surface area to volume ratio, which can reduce pyrolysis temperatures. The efficiency and completeness of the conversion may suffer as a result [24]. Larger particle sizes can boost char formation and increase fines output, which can reduce the process's overall efficiency [67]. Moreover, reduced throughput and increased energy consumption might result from larger particle sizes since they necessitate longer residence times in the reactor to achieve complete conversion [68].

Data from the current study broadly agree with trends seen in prior research when compared to similar studies in the literature. An increase in bio-oil yield and carbon conversion efficiency were observed when particle size was reduced from 6 mm to 0.5 mm in a research of fast pyrolysis of corn stover, suggesting greater overall energy efficiency [69]. Similar results were obtained in a research of fast pyrolysis of lignocellulosic biomass, where a reduction in particle size from 9.25 mm to 1.52 mm increased bio-oil yield and quality, indicating greater overall energy and total exergy efficiency [70].

4. Conclusions

This study aimed to investigate the impact of various pyrolysis operating parameters on the efficiency of the pyrolysis process, as well as the yields of its products, using MGW as the feedstock. The parameters under examination included temperature, holding time, and feedstock particle size. The findings of this study indicate that adjusting the temperature and holding time can have a positive effect on the yield of bio-oil, as well as the overall energy efficiency and total exergy efficiency of the pyrolysis process. However, it's important to note that these improvements have limits. For instance, when the temperature was set at 550 °C and the holding time at 4 min, an overall energy efficiency of 67.35% and a total exergy efficiency of 66.38% were observed. Additionally, the yields of bio-oil and syngas were measured at 37.52% and 17.33%, respectively. Furthermore, the results demonstrate that the particle size of the feedstock significantly influences both the overall efficiency of the process and the yields of its products. Smaller particle sizes resulted in greater yields and improved efficiency. For example, at a feedstock particle size of 2 mm, a temperature of 550 °C, and a holding time of 3 min, a bio-oil yield of 37.12%, a syngas yield of 15.63%, an overall energy efficiency of 72.89%, and a total exergy efficiency of 68.4% were found.

Important implications for designing and optimising pyrolysis processes employing MGW as a feedstock are provided by this study. Higher yields and efficiency, which could lead to increased process economics and sustainability, may be attainable by carefully managing pyrolysis operation parameters and selecting optimum feedstock particle sizes. In addition, researchers and experts in the industry can benefit from this study's findings as they seek to enhance pyrolysis operations employing additional types of biomass feedstocks. While the results of this study are largely in line with those of other studies, it is important to note that more research is needed in several areas. The effect of other operating factors, such as heating rate and gas flow rate, on pyrolysis yields and efficiency could be investigated in future research. Also, additional study is required to properly comprehend the intricate relationship between different operational factors and how they affect pyrolysis yields and efficiency.

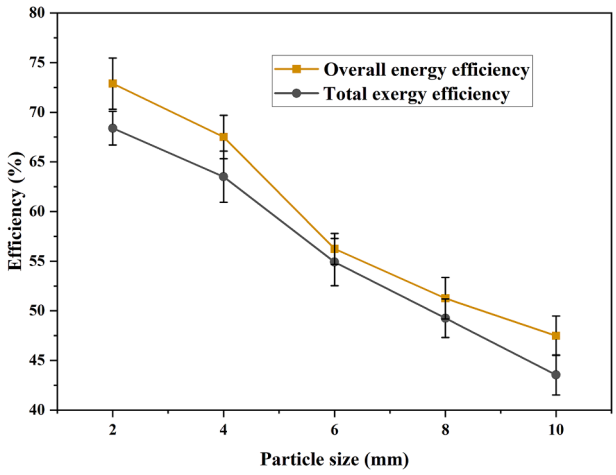

Fig. 8. The effect of particle size on overall energy efficiency and total exergy efficiency of the fast pyrolysis process of MGW.

Declaration of Competing Interest

The authors declare that they have no known competing financial interests or personal relationships that could have appeared to influence the work reported in this paper.

Data availability

Data will be made available on request.

Acknowledgements

The authors would like to acknowledge Fuel and Energy Research Group of the Central Queensland University for providing experimental and characterisation facilities.

Appendix A. Supplementary data

Supplementary data to this article can be found online at https://doi.org/10.1016/j.fuel.2023.129815.

References

[1] Owusu PA, Asumadu-Sarkodie S. A review of renewable energy sources, sustainability issues and climate change mitigation. Cogent Eng 2016;3(1):1167990.
[2] Ramos JL, Pakuts B, Godoy P, García-Franco A, Duque E. Addressing the energy crisis: using microbes to make biofuels. J Microbial Biotechnol 2022;15(4):1026–30.
[3] Kabir MJ, Chowdhury AA, Rasul MG. Pyrolysis of municipal green waste: a modelling, simulation and experimental analysis. Energies 2015;8(8):7522–41.
[4] Hasan MM, Rasul MG, Jahirul MI, Khan MMK. Characterization of pyrolysis oil produced from organic and plastic wastes using an auger reactor. Energ Conver Manage 2023;278:116723.
[5] Carpenter D, Westover TL, Czernik S, Jablonski W. Biomass feedstocks for renewable fuel production: a review of the impacts of feedstock and pretreatment on the yield and product distribution of fast pyrolysis bio-oils and vapors. Green Chem 2014;16(2):384–406.

[6] Sarwer A, Hussain M, AaH A-M, Inayat A, Rafiq S, Khurram MS, et al. Suitability of biofuels production on commercial scale from various feedstocks: a critical review. ChemBioEng Rev 2022;9(5):423–41.
[7] Zhang S, Wu Y, Wang Y, Zhong M, Wang G, Ban Y, et al. Facile demineralization of biochar and its catalytic upgrading of bio-oil from fast pyrolysis of bagasse. Fuel 2023;349:128714.
[8] Makepa DC, Chihobo CH, Musademba D. Advances in sustainable biofuel production from fast pyrolysis of lignocellulosic biomass. Biofuels 2023;14(5):529–50.
[9] Li M, Zhang YS, Cheng S, Qu B, Li A, Meng F, et al. The impact of heating rate on the decomposition kinetics and product distribution of algal waste pyrolysis with in-situ weight measurement. Chem Eng J 2023;457:141368.
[10] Iliopoulou EF, Pachatouridou E, Marianou AA, Michailof C, Kalogiannis KK, Lappas AA. Catalytic pyrolysis of olive mill wastes towards advanced bio-fuels and bio-chemicals using metal oxide catalysts. Catal Today 2023;420:114151.
[11] Zhang B, Zhong S, Fang J, Gao X, Wu S, Xu Q, et al. Valorization of water hyacinth biomass for bio-oil production using a novel combinatorial approach of UV/H2O2 advanced oxidation process pretreatment and catalytic fast pyrolysis over ZSM-5. Biomass Bioenergy 2023;175:106890.
[12] Ağbulut Ü, Sirohi R, Lichtfouse E, Chen W-H, Len C, Show PL, et al. Microalgae bio-oil production by pyrolysis and hydrothermal liquefaction: Mechanism and characteristics. Bioresour Technol 2023;376:128860.
[13] Campuzano F, Brown RC, Martínez JD. Auger reactors for pyrolysis of biomass and wastes. Renew Sustain Energy Rev 2019;102:372–409.
[14] Qi F, Wright MM. A DEM modeling of biomass fast pyrolysis in a double auger reactor. Int J Heat Mass Transf 2020;150:119308.
[15] Makkawi Y, Hassan Pour F, Elsayed Y, Khan M, Moussa O, Masek O, et al. Recycling of post-consumption food waste through pyrolysis: Feedstock characteristics, products analysis, reactor performance, and assessment of worldwide implementation potentials. Energ Conver Manage 2022;272:116348.
[16] Hasan MM, Rasul MG, Jahirul MI, Khan MMK. Fast pyrolysis of macadamia nutshell in an auger reactor: Process optimization using response surface methodology (RSM) and oil characterization. Fuel 2023;333:126490.
[17] Moreno-Sader K, Meramo-Hurtado SI, González-Delgado AD. Computer-aided environmental and exergy analysis as decision-making tools for selecting bio-oil feedstocks. Renew Sustain Energy Rev 2019;112:42–57.
[18] Parvez AM, Wu T, Afzal MT, Mareta S, He T, Zhai M. Conventional and microwave-assisted pyrolysis of gumwood: A comparison study using thermodynamic evaluation and hydrogen production. Fuel Process Technol 2019;184:1–11.
[19] Dincer I, Acar C. A review on clean energy solutions for better sustainability. Int J Energy Res 2015;39(5):585–606.
[20] Dorado AD, Baeza JA, Lafuente J, Gabriel D, Gamisans X. Biomass accumulation in a biofilter treating toluene at high loads – Part 1: Experimental performance from inoculation to clogging. Chem Eng J 2012;209:661–9.
[21] Wang X, Lv W, Guo L, Zhai M, Dong P, Qi G. Energy and exergy analysis of rice husk high-temperature pyrolysis. Int J Hydrogen Energy 2016;41(46):21121–30.
[22] Greco G, Di Stasi C, Rego F, González B, Manyà JJ. Effects of slow-pyrolysis conditions on the products yields and properties and on exergy efficiency: A comprehensive assessment for wheat straw. Appl Energy 2020;279:115842.
[23] Trubetskaya A, Grams J, Leahy JJ, Johnson R, Gallagher P, Monaghan RFD, et al. The effect of particle size, temperature and residence time on the yields and reactivity of olive stones from torrefaction. Renew Energy 2020;160:998–1011.
[24] Hong Z, Zhong F, Niu W, Zhang K, Su J, Liu J, et al. Effects of temperature and particle size on the compositions, energy conversions and structural characteristics of pyrolysis products from different crop residues. Energy 2020;190:116413.
[25] Hasan MM, Rasul MG, Ashwath N, Khan MMK, Jahirul MI. Fast pyrolysis of Beauty Leaf Fruit Husk (BLFH) in an auger reactor: Effect of temperature on the yield and physicochemical properties of BLFH oil. Renew Energy 2022;194:1098–109.
[26] Parvez AM, Mujtaba IM, Wu T. Energy, exergy and environmental analyses of conventional, steam and CO2-enhanced rice straw gasification. Energy 2016;94:579–88.
[27] Zhang Y, Li B, Li H, Liu H. Thermodynamic evaluation of biomass gasification with air in autothermal gasifiers. Thermochim Acta 2011;519(1):65–71.
[28] Tiara ES, Susanto Ginting A, Setiawan RPA, Joelianingsih, Tambunan AH. Exergy Analysis on Pyrolysis Process of Oil Palm Empty Fruit Bunch. IOP Conference Series: Materials Science and Engineering 2019;557(1):012058.
[29] Rahbari A, Venkataraman MB, Pye J. Energy and exergy analysis of concentrated solar supercritical water gasification of algal biomass. Appl Energy 2018;228:1669–82.
[30] Tang Y, Dong J, Chi Y, Zhou Z, Ni M. Energy and exergy analyses of fluidized-bed municipal solid waste air gasification. Energy Fuel 2016;30(9):7629–37.
[31] Zhang Y, Zhao Y, Gao X, Li B, Huang J. Energy and exergy analyses of syngas produced from rice husk gasification in an entrained flow reactor. J Clean Prod 2015;95:273–80.
[32] Zhang Y, Ji G, Ma D, Chen C, Wang Y, Wang W, et al. Exergy and energy analysis of pyrolysis of plastic wastes in rotary kiln with heat carrier. Process Saf Environ Prot 2020;142:203–11.
[33] Saidur R, BoroumandJazi G, Mekhilef S, Mohammed HA. A review on exergy analysis of biomass based fuels. Renew Sustain Energy Rev 2012;16(2):1217–22.
[34] Dewulf J, Van Langenhove H, Muys B, Bruers S, Bakshi BR, Grubb GF, et al. Exergy: its potential and limitations in environmental science and technology. Environ Sci Tech 2008;42(7):2221–32.
[35] Abu Bakar MS, Ahmed A, Jeffery DM, Hidayat S, Sukri RS, Mahlia TMI, et al. Pyrolysis of solid waste residues from Lemon Myrtle essential oils extraction for bio-oil production. Bioresour Technol 2020;318:123913.
[36] Mahadevan R, Adhikari S, Shakya R, Wang K, Dayton D, Lehrich M, et al. Effect of alkali and alkaline earth metals on in-situ catalytic fast pyrolysis of lignocellulosic biomass: a microreactor study. Energy Fuel 2016;30(4):3045–56.
[37] Kim SW, Koo BS, Lee DH. A comparative study of bio-oils from pyrolysis of microalgae and oil seed waste in a fluidized bed. Bioresour Technol 2014;162:96–102.
[38] Wang H, Male J, Wang Y. Recent advances in hydrotreating of pyrolysis bio-oil and its oxygen-containing model compounds. ACS Catal 2013;3(5):1047–70.
[39] Demiral İ, Atilgan NG, Şensöz S. Production of biofuel from soft shell of pistachio (*pistacia vera l.*). Chem Eng Commun 2008;196(1–2):104–15.
[40] Channiwala SA, Parikh PP. A unified correlation for estimating HHV of solid, liquid and gaseous fuels. Fuel 2002;81(8):1051–63.
[41] Munir S, Daood SS, Nimmo W, Cunliffe AM, Gibbs BM. Thermal analysis and devolatilization kinetics of cotton stalk, sugar cane bagasse and shea meal under nitrogen and air atmospheres. Bioresour Technol 2009;100(3):1413–8.
[42] Gómez N, Banks SW, Nowakowski DJ, Rosas JG, Cara J, Sánchez ME, et al. Effect of temperature on product performance of a high ash biomass during fast pyrolysis and its bio-oil storage evaluation. Fuel Process Technol 2018;172:97–105.
[43] Zhang H, Liu M, Yang H, Jiang H, Chen Y, Zhang S, et al. Impact of biomass constituent interactions on the evolution of char's chemical structure: An organic functional group perspective. Fuel 2022;319:123772.
[44] Bridgwater AV. Review of fast pyrolysis of biomass and product upgrading. Biomass Bioenergy 2012;38:68–94.
[45] Mettler MS, Vlachos DG, Dauenhauer PJ. Top ten fundamental challenges of biomass pyrolysis for biofuels. Energ Environ Sci 2012;5(7):7797–809.
[46] Tsai WT, Lee MK, Chang YM. Fast pyrolysis of rice husk: Product yields and compositions. Bioresour Technol 2007;98(1):22–8.
[47] Chen Y, Liang S, Xiao K, Hu J, Hou H, Liu B, et al. A cost-effective strategy for metal recovery from waste printed circuit boards via crushing pretreatment combined with pyrolysis: Effects of particle size and pyrolysis temperature. J Clean Prod 2021;280:124505.
[48] Luo S, Xiao B, Hu Z, Liu S. Effect of particle size on pyrolysis of single-component municipal solid waste in fixed bed reactor. Int J Hydrogen Energy 2010;35(1):93–7.
[49] Nurul Islam M, Nurul Islam M, Rafiqul Alam Beg M, Rofiqul IM. Pyrolytic oil from fixed bed pyrolysis of municipal solid waste and its characterization. Renew Energy 2005;30(3):413–20.
[50] Mani T, Murugan P, Abedi J, Mahinpey N. Pyrolysis of wheat straw in a thermogravimetric analyzer: Effect of particle size and heating rate on devolatilization and estimation of global kinetics. Chem Eng Res Des 2010;88(8):952–8.
[51] Shen J, Wang X-S, Garcia-Perez M, Mourant D, Rhodes MJ, Li C-Z. Effects of particle size on the fast pyrolysis of oil mallee woody biomass. Fuel 2009;88(10):1810–7.
[52] Yu J, Sun L, Berrueco C, Fidalgo B, Paterson N, Millan M. Influence of temperature and particle size on structural characteristics of chars from Beechwood pyrolysis. J Anal Appl Pyrol 2018;130:127–34.
[53] Qureshi KM, Kay Lup AN, Khan S, Abnisa F, Wan Daud WMA. Optimization of palm shell pyrolysis parameters in helical screw fluidized bed reactor: Effect of particle size, pyrolysis time and vapor residence time. Cleaner Engineering and Technology 2021;4:100174.
[54] Sarkar JK, Wang Q. Different pyrolysis process conditions of south asian waste coconut shell and characterization of gas, bio-char, and bio-oil. Energies 2020;13(8):1970.
[55] He M, Xu Z, Sun Y, Chan PS, Lui I, Tsang DCW. Critical impacts of pyrolysis conditions and activation methods on application-oriented production of wood waste-derived biochar. Bioresour Technol 2021;341:125811.
[56] Mohan D, Pittman CU, Bricka M, Smith F, Yancey B, Mohammad J, et al. Sorption of arsenic, cadmium, and lead by chars produced from fast pyrolysis of wood and bark during bio-oil production. J Colloid Interface Sci 2007;310(1):57–73.
[57] Zhou N, Zhou J, Dai L, Guo F, Wang Y, Li H, et al. Syngas production from biomass pyrolysis in a continuous microwave assisted pyrolysis system. Bioresour Technol 2020;314:123756.
[58] Li H, Xu Q, Xiao K, Yang J, Liang S, Hu J, et al. Predicting the higher heating value of syngas pyrolyzed from sewage sludge using an artificial neural network. Environ Sci Pollut Res 2020;27(1):785–97.
[59] Hoang AT, Ong HC, Fattah IMR, Chong CT, Cheng CK, Sakthivel R, et al. Progress on the lignocellulosic biomass pyrolysis for biofuel production toward environmental sustainability. Fuel Process Technol 2021;223:106997.
[60] Ramesh N, Murugavelh S. A cleaner process for conversion of invasive weed (Prosopis juliflora) into energy-dense fuel: kinetics, energy, and exergy analysis of pyrolysis process. Biomass Convers Biorefin 2022;12(8):3067–80.
[61] Baghel P, Sakhiya AK, Kaushal P. Influence of temperature on slow pyrolysis of Prosopis Juliflora: An experimental and thermodynamic approach. Renew Energy 2022;185:538–51.
[62] Rupesh S, Muraleedharan C, Arun P. Energy and exergy analysis of syngas production from different biomasses through air-steam gasification. Frontiers in Energy 2020;14(3):607–19.
[63] Krishnan RY, Manikandan S, Subbaiya R, Kim W, Karmegam N, Govarthanan M. Advanced thermochemical conversion of algal biomass to liquid and gaseous biofuels: A comprehensive review of recent advances. Sustainable Energy Technol Assess 2022;52:102211.
[64] Li J, Dou B, Zhang H, Zhang H, Chen H, Xu Y, et al. Pyrolysis characteristics and non-isothermal kinetics of waste wood biomass. Energy 2021;226:120358.

[65] Tripathi M, Sahu JN, Ganesan P. Effect of process parameters on production of biochar from biomass waste through pyrolysis: A review. Renew Sustain Energy Rev 2016;55:467–81.
[66] Peters JF, Petrakopoulou F, Dufour J. Exergetic analysis of a fast pyrolysis process for bio-oil production. Fuel Process Technol 2014;119:245–55.
[67] McKendry P. Energy production from biomass (part 3): gasification technologies. Bioresour Technol 2002;83(1):55–63.
[68] Al-Rumaihi A, Shahbaz M, McKay G, Mackey H, Al-Ansari T. A review of pyrolysis technologies and feedstock: A blending approach for plastic and biomass towards optimum biochar yield. Renew Sustain Energy Rev 2022;167:112715.
[69] Huang Y-F, Kuan W-H, Chang C-Y. Effects of particle size, pretreatment, and catalysis on microwave pyrolysis of corn stover. Energy 2018;143:696–703.
[70] Suriapparao DV, Vinu R. Effects of biomass particle size on slow pyrolysis kinetics and fast pyrolysis product distribution. Waste Biomass Valoriz 2018;9(3):465–77.